Study on Drug Release Behaviors of Poly-α,β-[*N*-(2-hydroxyethyl)-L-aspartamide]-*g*-poly(ϵ-caprolactone) Nano- and Microparticles

Zhi-Mei Miao, Si-Xue Cheng,* Xian-Zheng Zhang, and Ren-Xi Zhuo*

Key Laboratory of Biomedical Polymers of Ministry of Education, Department of Chemistry, Wuhan University, Wuhan 430072, P. R. China

Received March 3, 2006; Revised Manuscript Received March 23, 2006

Biodegradable amphiphilic graft copolymers poly-α,β-[N-(2-hydroxyethyl)-L-aspartamide]-*g*-poly(ϵ-caprolactone) (PHEA-*g*-PCL) with different branch lengths were synthesized through the ring-opening polymerization of ϵ-caprolactone initiated by the macroinitiator PHEA bearing hydroxyl groups. With use of the graft copolymers with different compositions, nanoparticle drug delivery systems with sizes smaller than 100 nm were prepared by a dialysis method, and microparticle drug delivery systems with sizes smaller than 5 μm were fabricated by a melting-emulsion method. The regularly spherical shapes of the drug-loaded nano- and microparticles were verified by transmission electron microscopy and scanning electron microscopy. In vitro drug release properties of nano- and microparticle drug delivery systems were investigated, with the emphasis on the effects of polymer composition, particle size, and drug-loading content on the release behaviors.

Introduction

Since emerging in the early 1970s, controlled drug delivery technology has attracted increasing attention with the aim of achieving the controlled, systematic, or site-specific drug release over an extended period of time. This technology offers numerous advantages compared to conventional therapeutic systems, by prolonging duration time, reducing side effects, retaining drug bioactivity, and thus improving the therapeutic efficiency.[1] A powerful approach for controlling drug delivery is to incorporate the drug into biodegradable polymeric nano- or microparticles, which can achieve a controlled and sustained fashion through the drug diffusion or/and the polymeric carrier degradation. The advantages of nano- or microparticle drug delivery systems are the injectable property which can avoid the inconvenient surgical insertion,[2,3] and the possibility to achieve passive targeting when their sizes are in particular ranges.[4,5]

The most widely studied biodegradable polymers for controlled drug delivery are aliphatic polyesters, such as polylactide, polyglycolide, poly(ϵ-caprolactone) (PCL), and their copolymers.[1,3,6−8] However, due to the hydrophobic nature of these polymers, when the size of their drug delivery systems reduces to the nanometer range, the nanoparticles are thermodynamically unstable and tend to aggregate. Furthermore, the hydrophobic nanoparticles are usually eliminated by the reticuloendothelial system after intravenous injection. To overcome these limitations, nanoparticles formed by the self-assembling of amphiphilic polymers are interestingly studied as drug carriers. The amphiphilic nanoparticles not only have good thermodynamic stability in aqueous solutions but also exhibit increased blood circulation time, which is critical for effective drug delivery. In the past decades, amphiphilic block copolymers have been extensively investigated. Compared with the block copolymers, amphiphilic graft copolymers can easily form micelles because of the possibility of forming micelles within one or several polymer chains. Moreover, since graft copolymers have multigrafted branches, the hydrophilic/hydrophobic balance can be readily controlled by adjusting the relative grafting density.[9] Another advantage of graft copolymers is that many reactive functional groups exist along each backbone, which allows further incorporation of various biorecognizable ligands to realize the positive targeted drug delivery and/or to achieve the enhanced cell adhesion and recognition. Because of these favorable properties, amphiphilic graft copolymers are of special interest as biomaterials.

In our previous work,[10] novel biodegradable amphiphilic graft copolymers with hydrophilic PHEA backbone and hydrophobic PCL side chains were synthesized through the ring-opening polymerization of ϵ-caprolactone (CL) initiated by the macroinitiator PHEA. PCL is extensively studied as a biodegradable polymer for biomedical applications due to its biocompatibility and high permeability to low molecular weight substances at body temperature. PHEA is a synthetic water-soluble polymer with protein-like structure, and has been interestingly explored in the biomedical fields because it is nontoxic, nonantigenic, nonteratogenic, and multifunctional.[11,12] With control of the feed ratio of the macroinitiator PHEA to the monomer CL, graft polymers with different hydrophobic branch lengths and different properties can be obtained.[10]

In this study, we fabricated nanoparticle and microparticle drug delivery systems and studied their drug release properties. The study on in vitro drug release shows the release of the drug can be effectively sustained by entrapping the drug in the nanoparticles and microparticles. Both nanoparticles and microparticles exhibit good thermodynamic stability during the release period.

Due to the amphiphilicity, graft copolymers can self-assemble into micelles in an aqueous environment. Thus, nanoparticle drug delivery systems were prepared by a dialysis method.

The conventional methodologies for microsphere fabrication include emulsion, precipitation, and spraying techniques. However, there are still many challenges associated with these

* Corresponding authors. Fax: +86-27-68754509. E-mail: pibmp@public.wh.hb.cn.

10.1021/bm060200o CCC: $33.50
Published on Web 05/06/2006

techniques. Of particular concern is the use of organic solvents. The existence of organic solvents may lead to loss of or reduction in bioactivity of some drugs. In addition, many organic solvents are toxic and a low-level exposure to residual organic solvents may lead to lasting toxic effects such as neurobehavioral deficit. The techniques for preparing microspheres in the absence of organic solvents are highly desirable. In this study, the microparticle drug delivery systems were fabricated by a melting-emulsion method. The so-called "melting-emulsion method", which is similar to the hot homogenization technique for the solid lipid nanoparticle production, was developed by our group to fabricate polymeric microparticle drug delivery systems.[13] In comparison with other conventional methods, the melting-emulsion method does not involve any organic solvent and is very rapid and convenient, offering good control over the size of microparticles. In the melting-emulsion method, the drug was dissolved or dispersed in the polymer melt, and then the mixture was immersed in hot water and extruded through a membrane filter with a certain pore size repeatedly to obtain a homogeneous emulsion. Subsequently, the microemulsion was injected into icy water to get solid microspheres. To be applicable to this method, the polymer should satisfy the requirements including proper melting point and relatively low viscosity. Most commonly, the molten viscosities of the linear polymers with relatively high molecular weights are much higher than the required value for microparticle fabrication using this method. This implies the molecular weight of the polymers should be in a certain range and/or the polymers should have some specific structures such as graft structure or hyperbranched structure which result in a low molten viscosity.[13,14] In our investigation, the graft copolymers were found to have lower viscosities and proper melting points, which can satisfy the fabrication requirements. Based on our studies on other amphiphilic graft copolymers with PHEA as the backbones and polylactide[15] or polyglycolide[16] as branches, we found their melting points are too high to be fabricated into microparticles using this melting-emulsion method.

Experimental Section

Materials. L-Aspartic acid and phosphoric acid were of analytical grade and used as supplied by Shanghai Chemical Co., China. Ethanolamine (Shanghai Chemical Co.) was distilled before use. *N*,*N*-Dimethylformamide (DMF) was purified by distillation over P_2O_5 and CaH_2. ϵ-Caprolactone (Aldrich) was dried over CaH_2 for 2 days and distilled under reduced pressure prior to use. Prednisone acetate was purified from prednisone acetate tablets (Zhejiang Xianju Pharmaceutical Co. Ltd., China). The prednisone acetate tablets were ground and dissolved in chloroform. Then the starch in the drug tablets was removed by filtration to get prednisone acetate after removal of the solvent.

Synthesis of PHEA-*g*-PCL Graft Copolymers. PHEA was synthesized according to a literature procedure.[17] PHEA-*g*-PCL copolymers were synthesized by bulk ring-opening polymerization of CL using PHEA with pendant hydroxyl groups as a macroinitiator without adding any catalyst.[10] PHEA and CL, with a specific feed ratio of the hydroxyl group in PHEA to the monomer CL (1/4 and 1/10 for PHEA-*g*-PCL-a and PHEA-*g*-PCL-b, respectively), were well mixed and transferred to a thoroughly dry silanized glass flask with a magnetic stirring bar. The flask was evacuated, purged with argon three times, and sealed, followed by immersion in an oil bath preheated to 200 °C for 5 min. Then the reaction was carried out at 120 °C for 48 h. After polymerization, the product was dissolved in dichloromethane and then precipitated in ether, subsequently isolated by centrifugation and dried under vacuum at room temperature.

Characterizations of PHEA-*g*-PCL Graft Copolymers. Fourier transform infrared (FTIR) spectra were obtained on a PerkinElmer-2 spectrometer. FTIR (KBr): 1725 cm^{-1} (C═O in PCL branch), 1660 cm^{-1} (C═O in PHEA backbone), and 1543 cm^{-1} (N−H in PHEA backbone).

^{1}H nuclear magnetic resonance (^{1}H NMR) spectra were recorded on a Mercury VX-300 spectrometer (300 MHz). ^{1}H NMR ($CDCl_3$): 1.22 ppm (PCL branch: $CH_2CH_2C\mathbf{H_2}CH_2CH_2$), 1.46 ppm (PCL branch: $CH_2C\mathbf{H_2}CH_2C\mathbf{H_2}CH_2$), 2.24 ppm (PCL branch: $COC\mathbf{H_2}$), 3.96 ppm (PCL branch: $C\mathbf{H_2}O$), 2.61 ppm (PHEA backbone: $CHC\mathbf{H_2}$-CONH), 3.14 ppm (PHEA backbone: $NHC\mathbf{H_2}CH_2OH$), 3.44 ppm (PHEA backbone: $CH_2C\mathbf{H_2}OH$), 4.50 ppm (PHEA backbone: NH-$C\mathbf{H}(CO)CH_2$), 3.32 ppm (PHEA backbone: $C\mathbf{H_2}CH_2OCO$), and 4.02 ppm (PHEA backbone: $CH_2C\mathbf{H_2}OCO$).

The molecular weights of graft copolymers were determined by combined size-exclusion chromatography and multiangle laser light scattering (SEC-MALLS) analysis. A dual detector system, consisting of a MALLS device (DAWN EOS, Wyatt Technology) and an interferometric refractometer (Optilab DSP, Wyatt Technology), was used. The SEC system (2690D, Waters) was equipped with a precolumn and two Shodex columns (K805 and K8025). $CHCl_3$ was used as an eluent. The polymer concentration was 3 mg/mL and the flow rate was 1 mL/min. The MALLS detector was operated at a laser wavelength of 690.0 nm.

The water uptake was measured after incubating the polymer films with a thickness of 0.5 mm in distilled water at 37 °C for 48 h. The water uptake was calculated as follows:

$$\text{water uptake} = (W_{\text{wet}} - W_{\text{dry}})/W_{\text{dry}} \times 100\%$$

The weight of the wet polymer film, W_{wet}, was measured gravimetrically after incubating the film in distilled water at 37 °C for 48 h. The weight of the dried polymer film, W_{dry}, was measured gravimetrically after drying the wet film that was incubated in distilled water for 48 h in a vacuum oven for 24 h.

The critical micelle concentration (CMC) values of graft copolymers were determined by fluorescence spectroscopy. Graft copolymer solutions were prepared as follows. Fifty milligrams of graft copolymers was dissolved in 2 mL of THF, and then distilled water was added slowly with agitation. After THF was removed under vacuum at room temperature, the solution was diluted to 50.0 mL. The resultant solution was adjusted to the various concentrations. To determine the CMC, pyrene was used as a fluorescent probe. A particular amount of pyrene in THF was added to each 10.0 mL volumetric flask. After the solvent THF was evaporated, 10 mL of the copolymer solution with a specific concentration was added to the flask. Then the solution was shaken at 37 °C for 3 h to equilibrate the pyrene and the micelles and cooled overnight to room temperature. The final concentration of pyrene was 6.0×10^{-7} M. Fluorescence spectra were recorded on a Shimadzu RF-5301 PC spectrofluorophotometer at the emission wavelength of 391 nm with excitation bandwidth of 5 nm and the emission bandwidth of 3 nm.

Preparation of Nano- and Microparticles. Polymeric nanoparticles containing prednisone acetate were prepared by a dialysis method. Briefly, 20 mg of graft copolymer and 10 mg of prednisone acetate were dissolved in 4 mL of DMF and stirred at room temperature for 30 min. To form drug-loaded micelles and remove free drug, the solution was dialyzed against 1.0 L of distilled water for 24 h, during which the water was renewed every 4 h. The suspension was then freeze-dried.

Drug-loaded microparticles were prepared by a melting-emulsion method.[13] One hundred fifty milligrams of graft copolymers and a particular amount of prednisone acetate were well mixed. The mixture was immersed in hot water at 80 °C with the presence of surfactant Tween 80 and then was extruded through a 0.45 μm membrane filter several times to obtain a homogeneous emulsion. Subsequently, the emulsion was injected into icy water through the 0.45 μm pore diameter membrane filter to get solid drug-loaded microparticles. The microparticles were then centrifuged and rinsed three times with distilled water to remove the un-entrapped drug.

Scheme 1. Chemical Structure of PHEA-*g*-PCL Graft Copolymers

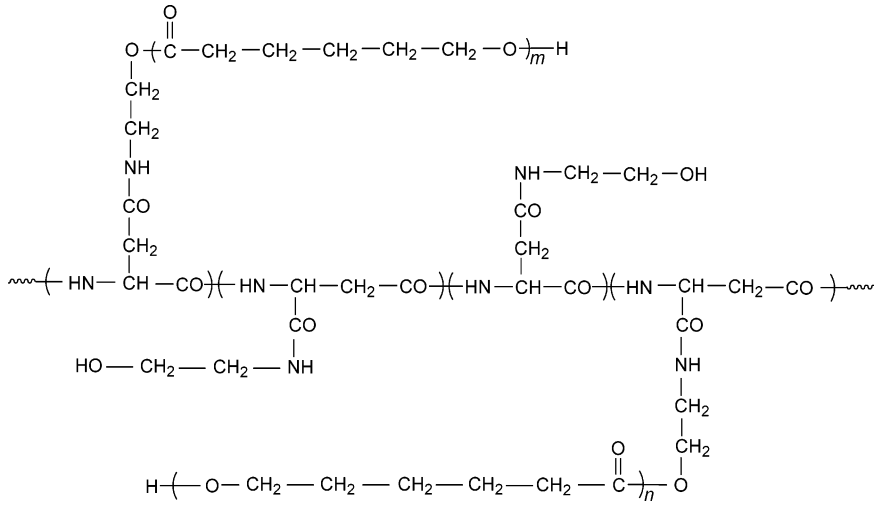

Table 1. Synthesis, Chemical Structure, and Molecular Weight of PHEA-*g*-PCL Graft Copolymers[10]

sample	−OH/CL feed ratio (mol/mol)	yield (%)	HEA/CL in polymer (mol/mol)[a]	unreacted −OH groups in PHEA backbone (%)[a]	mean number of CL units in each branch[a]	M_w[b]	M_w/M_n[b]
PHEA-*g*-PCL-a	1/4	75.8	1/4.88	55	10.8	18800	1.44
PHEA-*g*-PCL-b	1/10	83.8	1/15.67	45	28.5	24400	1.23

[a] Calculated from ^{1}H NMR. [b] Determined by SEC-MALLS.

Characterization of Nano- and Microparticles. To determine the drug-loading content and entrapment efficiency, the drug-loaded polymeric nano- or microparticles were dissolved in DMF. The prednisone acetate concentrations in the solutions were then determined by an ultraviolet−visible spectrophotometer (Perkin-Elmer Lambda Bio 40).

The weight loss of microparticles during degradation was measured gravimetrically. Twenty milligrams of blank microparticles without drug were immersed in 10 mL of phosphate buffer (PBS, 0.1 M, pH 7.4) at 37 °C. At predetermined time intervals, the samples were centrifuged, rinsed two times with distilled water, freeze-dried, and then weighed.

The drug-loaded nanoparticles were visualized by a JEOL JEM-100CXII transmission electron microscope (TEM) at an acceleration voltage of 80 kV. Before visualization, a droplet of nanoparticle suspension was placed on a copper grid with Formvar film and dried.

The drug-loaded microparticles were observed by an Hitachi X650 scanning electron microscope (SEM). The samples were prepared by placing a droplet of microparticle suspension onto a glass slide. The samples were then dried overnight and were sputter-coated with gold prior to being visualized.

The sizes of drug-loaded nanoparticles and microparticles were measured by a particle size analyzer (Beckman Coulter N_4 Plus).

In Vitro Drug Release Study. Five milligrams of drug-loaded nanoparticles or 10 mg of drug-loaded microparticles were suspended in 2 mL of PBS (0.1 M, pH 7.4) and then transferred into a dialysis bag. The dialysis bag was sealed and immersed into 8 mL of PBS. The system was shaken in a shaking water bath at 37 °C. At predetermined intervals, 3 mL of PBS solution was taken out and replaced by fresh PBS. The drug concentration was determined by measuring the absorbance at 243 nm in an ultraviolet−visible spectrophotometer (Perkin-Elmer Lambda Bio 40). The cumulative releases were determined by comparing the amount of the released drug and the total drug loading.

Results and Discussion

Synthesis and Properties of Graft Copolymers. The chemical structure of amphiphilic PHEA-*g*-PCL graft copolymers used as drug carriers is shown in Scheme 1. With the hydrophilic PHEA backbone and PCL hydrophobic side chains, PHEA-*g*-PCL copolymers exhibit amphiphilic properties. The copolymers were synthesized by ring-opening polymerization of ϵ-caprolactone using PHEA with hydroxyl groups as a macroinitiator without adding any catalyst.[10] The polymerization reaction was conducted under rigorously anhydrous conditions to avoid the initiation by water. With control of the feed ratio of the macroinitiator to the monomer, graft copolymers with different compositions and properties were prepared. Table 1 presents the chemical structure and molecular weight of the graft copolymers. In our study, we synthesized two copolymers with different hydrophobic branch lengths. The mean numbers of CL units in each branch for PHEA-*g*-PCL-a and PHEA-*g*-PCL-b are 10.8 and 28.5, respectively, which implies PHEA-*g*-PCL-a is more hydrophilic compared with PHEA-*g*-PCL-b.

Table 2. Properties of PHEA-*g*-PCL Graft Copolymers[a]

sample	T_m (°C)	ΔH_m (J/g)	X_c (%)	water uptake (wt %)	CMC (mg/L)
PHEA-*g*-PCL-a	50.8	20.8	19.6	10.7	7.9
PHEA-*g*-PCL-b	52.0	45.3	36.2	2.7	5.0

[a] T_m, ΔH_m, and X_c were determined by DSC.[10]

The properties including T_m, crystallinity, and water uptake of graft copolymers are listed in Table 2. According to our previous studies, PHEA-*g*-PCL-a and PHEA-*g*-PCL-b are crystalline materials, which are ascribed to the crystallization of PCL branches.[10] The crystallinities of PCL components are listed in Table 2. Due to the incorporation of amorphous PHEA, both T_m and crystallinity of graft copolymers, which decrease with the increasing PHEA content in the copolymer, are lower than that of homopolymer PCL ($T_m = 60.6$ °C and $X_c = 62.6\%$). As shown in Table 2, the water uptake of PHEA-*g*-PCL-a is obviously higher than that of PHEA-*g*-PCL-b because the former has a higher content of the hydrophilic PHEA backbone.

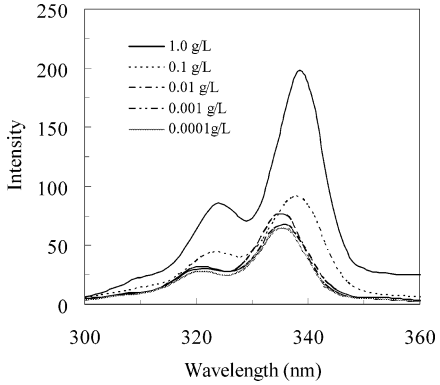

Figure 1. Fluorescence excitation spectra of pyrene in PHEA-*g*-PCL-a solutions with different concentrations.

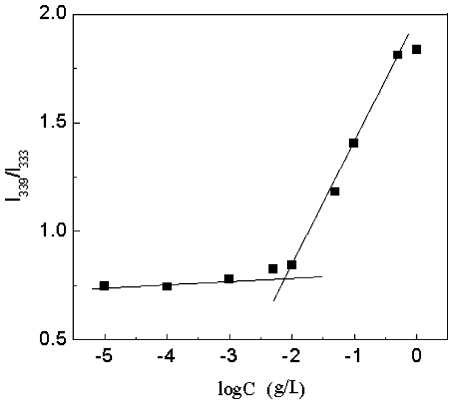

Figure 2. Plot of the intensity ratio I_{339}/I_{333} from pyrene excitation spectra vs log *C* of PHEA-*g*-PCL-a in distilled water.

The CMC of amphiphilic graft copolymers was evaluated by the fluorescence spectroscopy.[18,19] With use of PHEA-*g*-PCL-a as an example, Figure 1 shows the fluorescence spectra of pyrene in PHEA-*g*-PCL-a solutions with various concentrations. A red shift of pyrene in the excitation spectrum was observed with an increase in copolymer concentration, which is due to the preferential partition of pyrene into the hydrophobic PCL segments. The intensity ratio of I_{339}/I_{333} against PHEA-*g*-PCL-a concentration is plotted in Figure 2. The ratio increases slightly with increasing concentration at the low concentration range and increases rapidly above a certain concentration. The CMC value was determined from the intersection of two tangents to the parts of the curve corresponding to the left and right sides of the inflection point. The CMC values for PHEA-*g*-PCL-a and PHEA-*g*-PCL-b are 7.9 and 5.0 mg/L (Table 2), respectively, decreasing as the length of hydrophobic PCL segment increases.

Preparation and Characterization of Nano- and Microparticles. As the graft copolymers we prepared are amphiphilic, the dialysis method was chosen to fabricate drug-loaded nanoparticles. In our study, two types of nanoparticles, PHEA-*g*-PCL-a NP and PHEA-*g*-PCL-b NP, were prepared through self-assembly of PHEA-*g*-PCL-a and PHEA-*g*-PCL-b, respectively, in aqueous solutions.

To fabricate microparticles, the melting-emulsion method, which does not involve any organic solvent, was used. Because of the relatively low melting temperatures and viscosities, PHEA-*g*-PCL graft copolymers well satisfy the requirements of using the melting-emulsion method to fabricate microparticles. To investigate the effect of drug-loading content on the drug release behavior, different drug/polymer feed ratios of 1/10 and 1/20 were used to fabricate PHEA-*g*-PCL-a microparticles.

Table 3. Preparation and Properties of PHEA-*g*-PCL Nano- and Microparticles[a]

sample	drug/polymer feed ratio (w/w)	drug-loading content (wt %)	entrapment efficiency (%)	particle size (nm)	particle yield (%)
PHEA-*g*-PCL-a NP	1/2	3.3	5.7	32.4	57.7
PHEA-*g*-PCL-b NP	1/2	3.6	5.9	37.3	54.2
PHEA-*g*-PCL-a MP-1	1/10	7.3	46.5	2211.8	57.8
PHEA-*g*-PCL-a MP-2	1/20	2.5	31.4	2286.1	61.5
PHEA-*g*-PCL-b MP	1/20	2.2	23.5	2941.9	50.9

[a] Nanoparticles (NPs) were prepared by a dialysis method. Microparticles (MPs) were fabricated by a melting-emulsion method.

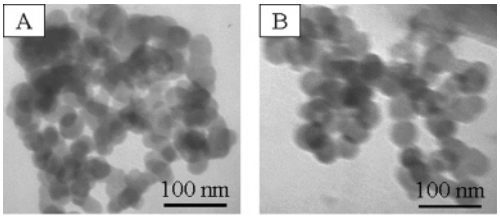

Figure 3. TEM images of nanoparticles before degradation. (A) PHEA-*g*-PCL-a NP and (B) PHEA-*g*-PCL-b NP.

Table 4. Weight Loss of Blank PHEA-*g*-PCL Microparticles during Degradation in PBS (0.1 M, pH = 7.4)

	weight loss (wt %)	
sample	48 h	240 h
PHEA-*g*-PCL-a	7.7	13.2
PHEA-*g*-PCL-b	1.0	3.8

The detailed preparation condition, drug-loading content, and entrapment efficiency of polymeric particle drug delivery systems are listed in Table 3. For nanoparticles, which encapsulate hydrophobic prednisone acetate by hydrophobic interaction, the drug-loading content and entrapment efficiency increase with the increase of hydrophobic PCL branch length. As shown in Table 3, in comparison with nanoparticles prepared by the dialysis method, the microparticles prepared by the melting-emulsion method exhibit considerably higher entrapment efficiencies. As listed in Table 3, the mean diameters of nanoparticles and microparticles are in the ranges of 30−40 nm and 2−3 μm, respectively. For both nano- and microparticles, with the increase of PCL side chain length, the particle sizes slightly increase.

The weight losses of microparticles during hydrolytic degradation are listed in Table 4. Compared with PHEA-*g*-PCL-a microparticles, PHEA-*g*-PCL-b microparticles show lower weight loss values because of its higher hydrophobic PCL content. The trend is in accordance with our previous study on the degradation of thin films of PHEA-*g*-PCL graft polymers.[10] The weight loss of nanoparticles is difficult to be measured because the weight of nanoparticles during degradation cannot be determined accurately due to the small size of nanoparticles.

The morphologies of nanoparticles were visualized by TEM. As shown in Figure 3, the size of nanoparticles before degradation is in good agreement with the results of the particle size analyzer. The two types of nanoparticles have good thermodynamic stability. Even after 240 h of degradation, nanoparticles still can be clearly observed under TEM (Figure 4). After degradation, the PHEA-*g*-PCL-a NP shows a reduced size, and PHEA-*g*-PCL-b NP does not exhibit an obvious size change. This phenomenon is explainable because copolymer PHEA-*g*-PCL-a has a faster degradation rate compared with copolymer PHEA-*g*-PCL-b.

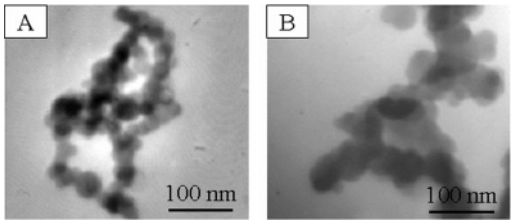

Figure 4. TEM images of nanoparticles after 240 h of degradation. (A) PHEA-*g*-PCL-a NP and (B) PHEA-*g*-PCL-b NP.

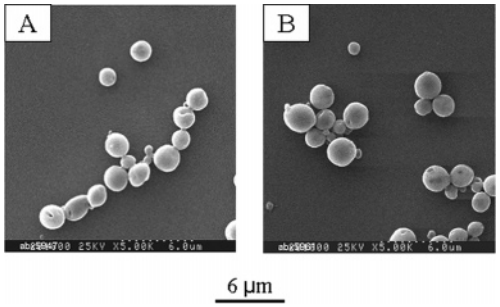

Figure 5. SEM images of microparticles before degradation. (A) PHEA-*g*-PCL-a MP-2 and (B) PHEA-*g*-PCL-b MP.

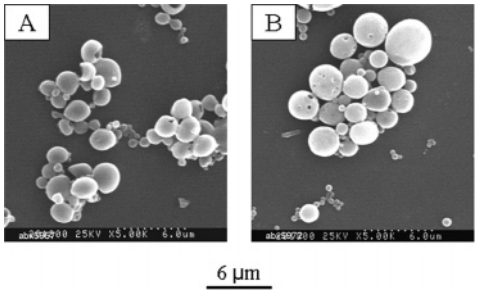

Figure 6. SEM images of microparticles after 240 h of degradation. (A) PHEA-*g*-PCL-a MP-2 and (B) PHEA-*g*-PCL-b MP.

The morphologies of microparticles were visualized by SEM. As demonstrated in Figure 5, the microparticles fabricated by the melting-emulsion method show a narrower distribution and a smaller size than that prepared by the traditional hot-melt technique.[20−22] The convenient melting-emulsion method was proved to be effective to control the size of the microparticles. The morphologies of microparticles after degradation are shown in Figure 6. For PHEA-*g*-PCL-a MP-2, the distortion of microparticles can be observed. The relatively fast degradation rate and higher water uptake are the main reasons that cause the distortion of PHEA-*g*-PCL-a MP-2. For PHEA-*g*-PCL-b MP with a slower degradation, no obvious morphology change can be detected.

In Vitro Drug Release Behaviors of Drug-Loaded Nano- and Microparticles. The in vitro release profiles of prednisone acetate from polymeric nanoparticles are shown in Figure 7. At the beginning of the drug release process, the burst release can be observed, which may be ascribed to the dissolution of the free drug absorbed on the surface of nanoparticles. With similar drug-loading content (3.3 wt % for PHEA-*g*-PCL-a NP and 3.6 wt % for PHEA-*g*-PCL-b NP), PHEA-*g*-PCL-a NP exhibits a faster release rate than PHEA-*g*-PCL-b NP. This is reasonable because the former has a higher hydrophilicity and a smaller size, which are beneficial to the diffusion of drug from polymeric particles. Since prednisone acetate is a hydrophobic drug, the stronger hydrophobic interaction between the drug and the polymer matrix PHEA-*g*-PCL-b is also a reason leading to a slower release rate for PHEA-*g*-PCL-b NP.

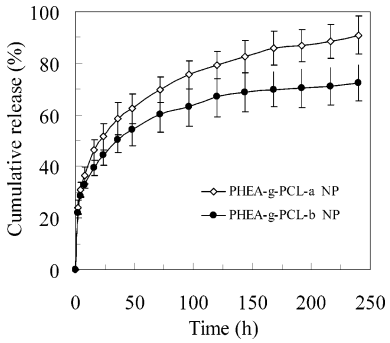

Figure 7. Release profile of prednisone acetate from nanoparticles of PHEA-*g*-PCL-a NP and PHEA-*g*-PCL-b NP in PBS (0.1 M, pH 7.4).

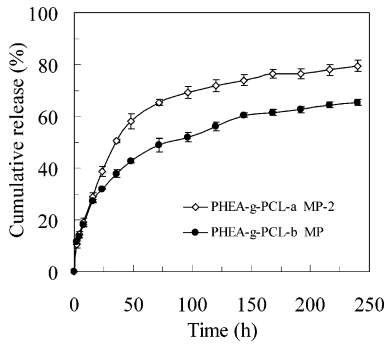

Figure 8. Release profile of prednisone acetate from microparticles of PHEA-*g*-PCL-a MP-2 and PHEA-*g*-PCL-b MP in PBS (0.1 M, pH 7.4).

Figure 8 presents the release profiles of prednisone acetate from PHEA-*g*-PCL-a MP-2 and PHEA-*g*-PCL-b MP with the same drug/polymer feed ratio of 1/20. Compared with nanoparticles, the initial burst release is not so obvious for microparticles. Taking account of the effect of hydrophilicity on the release behavior, a similar trend was observed for microparticles. PHEA-*g*-PCL-a MP-2 has a faster release rate compared with PHEA-*g*-PCL-b MP, indicating the drug release rate decreases with the increasing hydrophobic PCL content. As expected, microparticles exhibit slower release rates compared with nanoparticles, which is due to the decreased surface/volume ratio and the increased diffusion pathway which leads to the decreased concentration gradients (the driving forces for diffusion).

The release profiles of prednisone acetate from PHEA-*g*-PCL-a microparticles with different drug-loading content levels (7.3 wt % for PHEA-*g*-PCL-a MP-1 and 2.5 wt % for PHEA-*g*-PCL-a MP-2, respectively) are shown in Figure 9. Compared with PHEA-*g*-PCL-a MP-2, PHEA-*g*-PCL-a MP-1 with a high drug loading has a faster release rate for the amount of cumulative release.

As we know, the drug release from a degradable polymeric matrix is a very complicated process. Generally, several mechanisms, such as diffusion of the drug molecules and erosion of the polymer matrix, may be responsible for the overall release of a drug from a degradable polymeric matrix.[1] The relative importance of these mechanisms for the overall release rate varies considerably from one system to another, depending on the composition, molecular weight, hydrophilicity, crystallinity, and degradation rate of the polymer matrix and the size, porosity, and surface character of the drug delivery system. To simplify the release profile analysis, a classic empirical exponential expression (be applicable to the first 60% of fractional release) was established by Peppas et al. to describe the release behavior

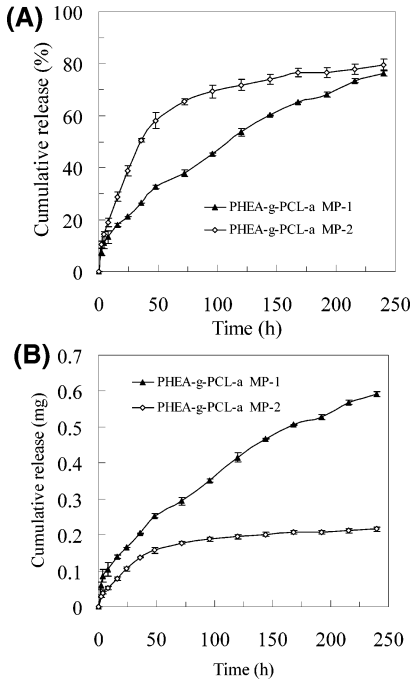

Figure 9. (A) Percentage of cumulative release and (B) amount of cumulative release of prednisone acetate from microparticles with different drug-loading contents in PBS (0.1 M, pH 7.4). The drug-loading content of PHEA-*g*-PCL-a MP-1 was 7.3 wt %, and the drug-loading content of PHEA-*g*-PCL-a MP-2 was 2.5 wt %.

of drug release systems with different mechanisms and various geometries:[23,24]

$$M_t/M_\infty = kt^n \quad (1)$$

where M_t and M_∞ are the cumulative drug release at time t and infinite time, k is a constant relating to the properties of the matrix and the drug, structural, and geometric characteristics of the device, and n is the release exponent, depending on the release mechanism and the geometry of the device. If Fickian diffusion occurs, n equals 0.5/0.45/0.43 for slab/cylinder/sphere. If non-Fickian (anomalous) diffusion dominates, the n value is between the above value corresponding to the Fickian diffusion and the value corresponding to zero-order release ($n = 1$) for nonswellable systems or case-II transport ($n = 1/0.89/0.85$ for slab/cylinder/sphere) for swellable systems.[23,24] So through determination of n value, the drug release mechanism can be identified. It should be noted that the n value is also affected by the size distribution of the drug release device. In comparison with the release behavior from a sample with monodispersity, the presence of a particle size distribution causes a substantial acceleration of the transport at early times and a marked retardation of the transport for longer times, leading to a lower n value compared with the value 0.43 for spheres with monodispersed size distribution if Fickian diffusion dominates.[23] When considering the degradation of polymer matrixes, the status becomes complicated. As the polymer begins to lose mass, the release rate accelerates because of the overall effect of diffusion and simultaneous polymer degradation, resulting in an increased n value.

We carried out the least-squares fit for the release data of microparticles using the exponential expression. The fitting data are shown in Table 5. The values of n for PHEA-*g*-PCL-a MP-1 and PHEA-*g*-PCL-a MP-2 are higher than 0.43, while the n for PHEA-*g*-PCL-b MP is slightly lower than 0.43. The results are reasonable if we consider the overall effect of several factors.

Table 5. Values of the Rate Constant (k), Release Exponent (n), and Correlation Coefficient (R^2) for PHEA-*g*-PCL Microparticles[a]

sample	k	n	R^2
PHEA-*g*-PCL-a MP-1	5.1575	0.4749	0.9895
PHEA-*g*-PCL-a MP-2	6.6859	0.5497	0.9903
PHEA-*g*-PCL-b MP	8.3408	0.4075	0.9914

[a] The parameter values were fitted using an exponent equation by Excel software.

For the current system, the polymer matrixes are amphiphilic polymers with detectable hydrolytic degradation rates during the release period and the release is controlled by the combined mechanism of diffusion and degradation that occur simultaneously, which results in an increased n, while the size distribution of microparticles leads to a reduced n. For PHEA-*g*-PCL-a with a relatively high degradation rate, the influence of polymer degradation is more dominant compared with the effect of size polydispersity. As an overall result, the fitted n values of PHEA-*g*-PCL-a MP-1 and PHEA-*g*-PCL-a MP-2 are higher than 0.43, while for PHEA-*g*-PCL-b with a relatively low degradation rate, the size polydispersity plays a critical role, leading to n lower than 0.43.

For nanoparticle drug delivery systems prepared by self-assembly of amphiphilic copolymers, it is somewhat difficult to use a mathematic model to accurately describe the release behavior because of the heterogeneous and complicated structure of the micelles.

Conclusions

Biodegradable amphiphilic graft copolymers poly-α,β-[*N*-(2-hydroxyethyl)-L-aspartamide]-*g*-poly(ϵ-caprolactone) were synthesized through the ring-opening polymerization of ϵ-caprolactone initiated by the macroinitiator PHEA. The CMC of the graft copolymers obtained by fluorescence spectroscopy decreases as the chain length of hydrophobic PCL increases. Drug-loaded nano- and microparticles based on biodegradable amphiphilic PHEA-*g*-PCL graft copolymers were successfully prepared, using the dialysis method and the convenient melting-emulsion method, respectively. The TEM and SEM images confirm the regularly spherical shapes of particles we fabricated. Compared with microparticles, the drug release rate of nanoparticles is faster, with a more obvious burst release. The release profiles of microparticles can be nicely fitted by the classical empirical exponential model. The drug release from microparticles is controlled by the combined degradation-diffusion mechanism.

Acknowledgment. This research was financially supported by National Natural Science Foundation of China (20474046) and "973 Programme" of the Ministry of Science and Technology of China (2005CB623903). One of the authors, Si-Xue Cheng, is grateful to the Ministry of Education of China for the financial support of "Trans-Century Training Programme Foundation for the Talents". Special thanks are due to Ms. Qing-Rong Wang for SEC-MALLS measurement.

References and Notes

(1) Edlund, U.; Albertsson, A. C. *Adv. Polym. Sci.* **2002**, *157*, 67.
(2) Jain, R. A. *Biomaterials* **2000**, *21*, 2475.
(3) Sinha, V. R.; Bansal, K.; Kaushik, R.; Kumria, R.; Trehan, A. *Int. J. Pharm.* **2004**, *278*, 1.
(4) Evora, C.; Soriano, I.; Rogers, R. A.; Shakesheff, K. M.; Hanes, J.; Langer, R. *J. Controlled Release* **1998**, *51*, 143.

(5) Akhtar, S.; Lewis, K. J. *Int. J. Pharm.* **1997**, *151*, 57.
(6) Soppimath, K. S.; Aminabhavi, T. M.; Kulkarni, A. R.; Rudzinski, W. E. *J. Controlled Release* **2001**, *70*, 1.
(7) Kissel, T.; Li, Y.; Unge, F. *Adv. Drug. Delivery Rev.* **2002**, *54*, 99.
(8) Peppas, L. B. *Int. J. Pharm.* **1995**, *116*, 1.
(9) Jeong, J. H.; Byun, Y.; Park, T. G. *J. Biomater. Sci. Polym. Ed.* **2003**, *14*, 1.
(10) Miao, Z. M.; Cheng, S. X.; Zhang, X. Z.; Zhuo, R. X. *Biomacromolecules* **2005**, *6*, 3449.
(11) Giammona, G.; Carlisi, B.; Palazzo, S. *J. Polym. Sci. Chem. Ed.* **1987**, *25*, 2813.
(12) Cavallaro, G.; Licciardi, M.; Giammona, G.; Caliceti, P.; Semenzato, A.; Salmaso, S. *J. Controlled Release* **2003**, *89*, 285.
(13) Yu, L.; Zhang, H.; Cheng, S. X.; Zhuo, R. X.; Li, H. *J. Biomed. Mater. Res. Part B: Appl. Biomater. B* **2006**, *77*, 39.
(14) Lang, M.; Wong, R. P.; Chu, C. C. *J. Polym. Sci., Part A: Polym. Chem.* **2002**, *40*, 1127.
(15) Peng, T.; Cheng, S. X.; Zhuo, R. X. *J. Biomed. Mater. Res. Part A* **2006**, *76*, 163.
(16) Peng, T.; Su, J.; Lin, G.; Cheng, S. X.; Zhuo, R. X. *Colloid. Polym. Sci.* **2006**, *284*, 834.
(17) Peng, T.; Cheng, S. X.; Zhuo, R. X. *J. Polym. Sci., Part A: Polym. Chem.* **2004**, *4*, 1356.
(18) Jeong, Y. I.; Cheon, J. B.; Kim, S. H.; Nah, J. W.; Lee, Y. M.; Sung, Y. K.; Akaike, T.; Cho, C. S. *J. Controlled Release* **1998**, *51*, 169.
(19) Lavasanifar, A.; Samuel, J.; Kwon, G. S. *Colloids Surf. B: Biointerface* **2001**, *22*, 115.
(20) Mathiowitz, E.; Langer, R. *J. Controlled Release* **1987**, *5*, 13.
(21) Lin, W. J.; Yu, C. C. *J. Microencapsulation* **2001**, *18*, 585.
(22) Lin, W. J.; Kang, W. W. *J. Microencapsulation* **2003**, *20*, 169.
(23) Ritger, P. L.; Peppas, N. A. *J. Controlled Release* **1987**, *5*, 23.
(24) Ritger, P. L.; Peppas N. A. *J. Controlled Release* **1987**, *5*, 37.

BM060200O